Analysis of Circular Microstrip Antenna with Perturbation Segments

Takafumi FUJIMOTO*, Kazumasa TANAKA, Mitsuo TAGUCHI
Dept. of Electrical Eng. & Computer Science, Nagasaki University
1-14 Bunkyo-machi, Nagasaki-shi, 852-8131, Japan

Introduction

The cavity model is a simple and efficient analytical method on the microstrip antenna (MSA). In the cavity model the wall admittance at the aperture has to be determined in advance. The accuracy of the wall admittance influences the input impedance and resonant frequency of antenna. Authors have proposed the formulation method on the wall admittance of arbitrarily shaped MSA and applied it to the circular MSA [1], elliptical MSA[2] and rectangular MSA[3]. The wall admittance is defined in terms of the magnetic field due to the equivalent magnetic current on the aperture. The magnetic field is derived by using Green's functions in the spectral domain in order to consider the influence of dielectric substrate.

In this paper, the wall admittance of circular MSA with perturbation segments is calculated by our proposed method and the antenna is analyzed by the cavity model. Although the wall susceptance was formulated by the capacitance of fringe field around the aperture in previous studies[4][5], the susceptance given by our method consists of capacitance and inductance. The numerical results are presented which show that the susceptance of the primary mode in the neighborhood of the resonant frequency is inductive at the aperture of the perturbation segment and capacitive at the aperture except the perturbation segment.

Theory

Fig. 1 shows the circular MSA with perturbation segments and its coordinate system. The dimensions of the two perturbation segments are $b_0 \leq r \leq a_0$; $\phi = -\phi_1 \sim \phi_1$ and $\phi = \pi - \phi_1 \sim \pi + \phi_1$, respectively. The antenna is excited at $(d_0\ ,\ \phi_0)$ by a coaxial feeder through the dielectric substrate. The relative dielectric constant of substrate is ε_r.

The electromagnetic fields within and outside the cavity are denoted by $\boldsymbol{E}^d$, $\boldsymbol{H}^d$; $\boldsymbol{E}^e$, $\boldsymbol{H}^e$, respectively. The thickness of the substrate is assumed to be relatively small compared with the wavelength, so the electromagnetic fields within the cavity do not vary along the z direction. The internal fields $\boldsymbol{E}^d$ is expressed by the eigenfunctions in the cylindrical coordinate system as follows.

In Region 1

$$\boldsymbol{E}^d = \sum_{n=1}^{N} (E_{zn}^{cJ} + E_{zn}^{sJ})\boldsymbol{i}_z \tag{1}$$

$$E_{zn}^{cJ} = A_n J_n(k_1 r)\cos(n\phi) \quad , \quad E_{zn}^{sJ} = B_n J_n(k_1 r)\sin(n\phi) \tag{2}$$

In Region 2

$$\boldsymbol{E}^d = \sum_{n=1}^{N} (E_{zn}^{cJ} + E_{zn}^{sJ} + E_{zn}^{cN} + E_{zn}^{sN})\boldsymbol{i}_z \tag{3}$$

0-7803-4478-2/98/$10.00 (c) 1998 IEEE

$$E_{zn}^{cJ} = C_n J_n(k_1 r)\cos(n\phi) \quad , \quad E_{zn}^{cN} = D_n N_n(k_1 r)\cos(n\phi) \tag{4}$$

$$E_{zn}^{sJ} = E_n J_n(k_1 r)\sin(n\phi) \quad , \quad E_{zn}^{sN} = F_n N_n(k_1 r)\sin(n\phi) \tag{5}$$

where $J_n(k_1 r)$ and $N_n(k_1 r)$ are Bessel and Neumann functions of order n, respectively. $\{A_n\}$ - $\{F_n\}$ are unknown coefficients to be determined from the continuity conditions of the electromagnetic fields between the region 1 and 2 and the impedance boundary condition at the aperture[6]. Since the radiations from the aperture 2 and 4, 6 and 8 are cancelled each other, the magnetic currents on these apertures don't contribute to the radiation field. Therefore, the impedance boundary condition is applied as follows,

$$\int_{S_1+S_3+S_5+S_7} \{\sum_{n=1}^{N}(y_n^{cJ} E_{zn}^{cJ} + y_n^{cN} E_{zn}^{cN} + y_n^{sJ} E_{zn}^{sJ} + y_n^{sN} E_{zn}^{sN}) + H_\phi^d\} dS' = 0. \tag{6}$$

The wall admittances y_n^{cJ}, y_n^{cN}, y_n^{sJ} and y_n^{sN} are defined by the magnetic fields $H_{\phi n}^{cJ}$, $H_{\phi n}^{cN}$, $H_{\phi n}^{sJ}$ and $H_{\phi n}^{sN}$ produced by the equivalent magnetic current $M_n^{cJ}(= E_{zn}^{cJ})$, $M_n^{cN}(= E_{zn}^{cN})$, $M_n^{sJ}(= E_{zn}^{sJ})$ and $M_n^{sN}(= E_{zn}^{sN})$ on the aperture, respectively.

$$y_n^{cJ} = -\frac{H_{\phi n}^{cJ}}{M_n^{cJ}},\ y_n^{cN} = -\frac{H_{\phi n}^{cN}}{M_n^{cN}},\ y_n^{sJ} = -\frac{H_{\phi n}^{sJ}}{M_n^{sJ}},\ y_n^{sN} = -\frac{H_{\phi n}^{sN}}{M_n^{sN}} \tag{7}$$

The magnetic fields $\boldsymbol{H}^e$ at any point on the aperture produced by the magnetic current $\boldsymbol{M}(= M\boldsymbol{i}_\phi)$ are expressed as the following equation[1]-[3],

$$\begin{aligned}\boldsymbol{H}^e = -j\omega &\int_{S_1+S_3+S_5+S_7} (\boldsymbol{i}_X G_F^{XX} + \boldsymbol{i}_Y G_F^{YX}) M\, dS' \\ &+ \frac{1}{j\omega}\int_{S_1+S_3+S_5+S_7} (\nabla G_V)(\nabla' \cdot \boldsymbol{M})\, dS'\end{aligned} \tag{8}$$

where for the reason mentioned above, the magnetic currents on the aperture 2, 4, 6 and 8 are neglected. Green's functions G_F^{XX}, G_F^{YX} and G_V in the spatial domain are obtained by applying the inverse Fourier transform to Green's functions in the spectral domain [1]-[3].

Results and Discussion

Fig. 2 shows the calculated wall admittances y_1^{cJ} and y_1^{sJ} of the primary mode at the resonant frequency. In this paper, the discussions on y_1^{cN} and y_1^{sN} are omitted because y_1^{cN} and y_1^{sN} have the same characteristics as y_1^{cJ} and y_1^{sJ}. The calculated wall conductances g_1^{cJ} and g_1^{sJ} are constant in the aperture 1 and 3, respectively.

Substituting eqn.(8) into eqn.(7), the wall susceptance b_n^{cJ} is expressed as follows,

$$b_n^{cJ} = j\omega C_n - \frac{j}{\omega L_n} \tag{9}$$

$$C_n = \frac{\mathrm{Re}\{\int_{S_1+S_3+S_5+S_7} (\boldsymbol{i}_\phi \cdot \boldsymbol{i}_X G_F^{XX} + \boldsymbol{i}_\phi \cdot \boldsymbol{i}_Y G_F^{YX}) M_n^{cJ}\, dS'\}}{M_n^{cJ}} \tag{10}$$

$$L_n = \frac{M_n^{cJ}}{\mathrm{Re}\{\int_{S_1+S_3+S_5+S_7} (\boldsymbol{i}_\phi \cdot \nabla G_V)(\nabla' \cdot \boldsymbol{i}_\phi M_n^{cJ})\, dS'\}}. \tag{11}$$

b_n^{sJ} is given by replacing M_n^{cJ} in eqns.(9)-(11) by M_n^{sJ}. Eqns.(9)-(11) indicate that the wall susceptance is equivalent to LC parallel circuit and C and L correspond to

vector and scalar potentials, respectively. As shown in Fig. 2, the wall susceptance b_1^{cJ} is capacitive at the apertures 1 and 3. b_1^{sJ} is inductive at the aperture 1 and capacitive at the aperture 3.

Fig. 3 shows the frequency characteristics of b_1^{cJ} at $\phi = 0°$ and b_1^{sJ} at $\phi = 90°$, which influence the electromagnetic fields within the antenna cavity. b_1^{cJ} and b_1^{sJ} vary from inductive to capacitive as the frequency becomes higher.

Fig. 4 shows the frequency characteristics of calculated input impedances of circular MSA with perturbation segments. The resonant frequencies are 6.59GHz and the minimum axial ratio is 0.07dB at 6.554GHz.

Conclusion

The wall admittance of circular MSA with perturbation segments is evaluated by using Green's functions in the spectral domain. The wall susceptances can be regarded as the LC parallel circuit. In neighborhood of the resonant frequency, the wall susceptance of the primary mode is inductive at the aperture of the perturbation segment and is capacitive at the aperture except the perturbation segment.

The input impedances and axial ratios are calculated by the cavity model with this wall admittances and the geometry of the patch to radiate circular polarization is determined. The comparison between the numerical and the measured ones will be reported at the Symposium site.

Acknowledgment

This research was supported in part by Grant-in-Aid for Scientific Research 09750429 from the Ministry of Education, Science and Culture of Japan.

References

[1] T.Fujimoto, M.Taguchi and K.Tanaka : "Surface admittance of circular microstrip antenna", *Proc. IEEE, AP-S, Int.,Symp.*, vol.1, pp.696-699, June 1995.

[2] T.Fujimoto, M.Taguchi and K.Tanaka : "Surface admittance of elliptical microstrip antenna", *Proc. of Int., Symp. on Antennas and Propagat.*, vol. 2, pp.541-544, Sep. 1996.

[3] T Mizuguchi, T.Fujimoto, K.Tanaka and M.Taguchi : "Surface admittance of rectangular microstrip antenna", *Proc. Technical report of IEICE*, vol. AP96-128, pp.65-70, Jan. 1997.

[4] L.C.Shen, S.A.Long, M.R.Allerding and M.D.Walton : "Resonant frequency of a circular disc, printed-circuit antenna", *IEEE Trans., Antennas Propagat.,*, vol. AP-25, pp.595-596, July 1977.

[5] W.C.Chew and J.A.Kong : "Effects of fringing fields on the capacitance of circular microstrip disk", *IEEE Trans., Microwave Theory Tech.*, vol. MTT-28, no.2, pp.98-103, Feb. 1980.

[6] L.C.Shen : "Analysis of circular-disc printed-circuit antenna", *Proc. IEE*, vol. 126, no.12, pp.1220-1222, Dec. 1979.

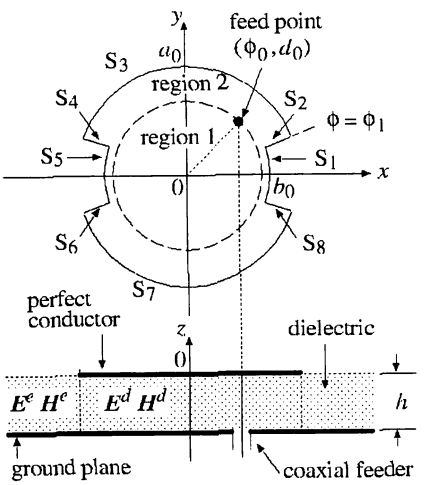

Fig. 1 Circular MSA with perturbation segments

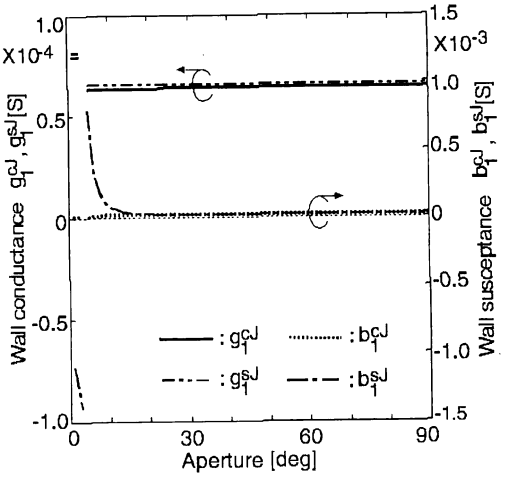

Fig. 2 Calculated wall admittances distribution at apertures

a_0=9.0mm, b_0=6.7mm, h=0.764mm, ε_r=2.15, ϕ_1=4°, frequency=6.59GHz

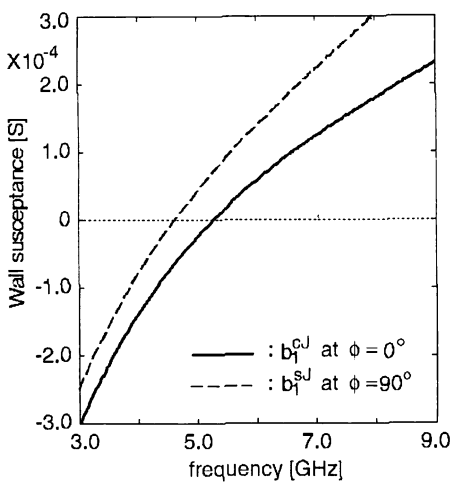

Fig. 3 Frequency characteristics of calculated wall susceptances

a_0=9.0mm, b_0=6.7mm, h=0.764mm, ε_r=2.15, ϕ_1=4°

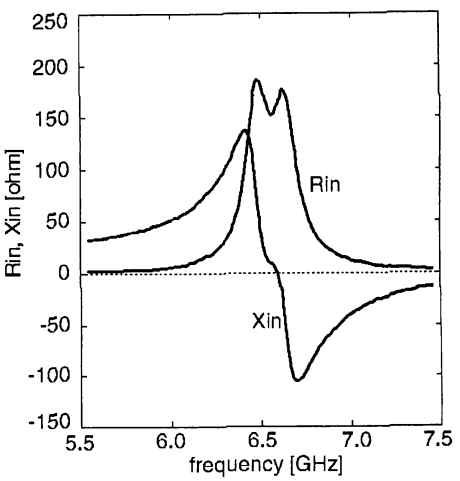

Fig. 4 Frequency characteristics of calculated input impedance

a_0=9.0mm, b_0=6.7mm, h=0.764mm, ε_r=2.15, ϕ_1=4°, d_0=6.0mm, ϕ_0=45°, N=5